Calculation of Stress Intensity Factor of Stress Corrosion Cracking in the Weldment of Core Shroud of Boiling Water Reactor

Yongkui Li
Japan Atomic Energy Agency

Yoshiyuki Kaji
Japan Atomic Energy Agency

Takahiro Igarashi
Japan Atomic Energy Agency

Key Words: *Stress intensity factor, Stress corrosion cracking Weld residual stress, Core shroud*

ABSTRACT

Stress corrosion cracking is recently observed in the heat affected zone of welded joint of the core shroud of boiling water reactors. Stress intensity factor is essential for evaluation of crack growth behavior in stress corrosion cracking. In this study, stress intensity factor of surface crack under residual stress field was calculated using two experienced equations in API RP579 with the aids of finite element method. The feasibility and reliability of the used methods were discussed.

1. INTRODUCTION

Stress corrosion cracking (SCC) is normally found in the core shroud of the boiling water reactor of a nuclear power plant after it has serviced several decades. Stress intensity factor estimated by using an appropriate modeling of components is essential for evaluation of crack growth behavior in stress corrosion cracking. For the appropriate modeling of welded components with a surface crack, it is important to understand the effects of residual stress distribution on the stress intensity factor of the crack.

In this study, the stress intensity factor of the SCC was estimated using the methods of semi-elliptical shape surface crack in API RP579 [1]. The guide of API provides two methods to calculate the stress intensity factor. The results of tension-compression-tension axial weld residual stress in weldment H6a of a core shroud by ABAQUS were used [2-4]. On the basic of the axial stress at the crack tip, we calculated the stress intensity factor, and made comparison of the estimated results by the two methods.

2. SIMULATION RESULTS OF WELD RESIDUAL AXIAL STRESS

As shown in Fig. 1, the core shroud is an open cylinder without inner pressure, and the global model containing girth seam H6a was cut from the core shroud. The global model is composed of 12 weld beads and base metal part, and composed of 9207 elements with type of 8-node trilinear displacement [2-3]. The weld beads were heated one by one with defining heat DFLUX in subroutine in ABAQUS. The maximum temperature of bead was no more than 1200°C, and the layer temperature was controlled smaller than 180°C. After the final beads cooling to the room temperature, the distribution of weld residual stress was obtained.

Ring part is the base metal region below the girth seam H6a. Weld residual stress only distributes partially in the ring part below the girth seam H6a in the path shown Fig. 2. The path is 6mm to weld line of H6a in distance, at which the axial stress of outer surface is largest. Therefore, we assumed that the crack grew up along the path from outside of the core shroud. The curve of axial residual stress in the path through the wall appears like a "V" shape, and the compression stress is produced in the center region of the measurement path in the model. More details of the simulation on the axial stress can be found in Ref. 3.

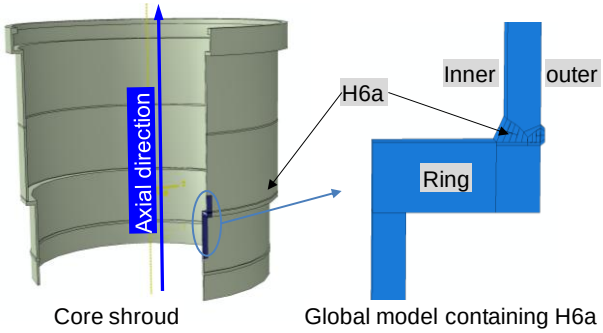

Fig. 1 Core shroud and the simulation global model containing girth seam H6a

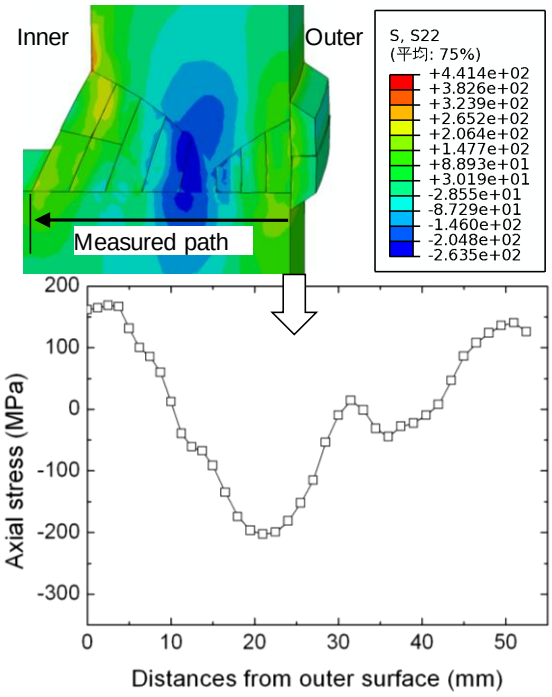

Fig. 2 Distribution of axial residual stress through the measured path in the ring part by simulation

3. CALCULATION METHODS FOR STRESS INTENSITY FACTOR

The SCC was assumed to initiate from the outer surface in

the ring part under the weld line of H6a seam. In views of convenience for constructing a surface crack, the ring part in the global model was cut in sub-model technology in ABAQUS. After that a semi-elliptical surface crack was introduced into the ring part as shown in Fig. 3, and the ratio of depth to half length (a/c) of crack was fixed by 0.5 with the growth of the crack. a and $2c$ are the depth and length of the introduced static crack in elliptical shape. Using the cracks with different depths, the stress intensity factor was calculated by two methods in the guide of API RP579.

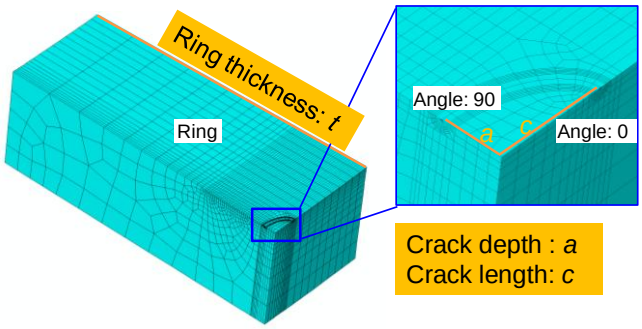

Fig. 3 Surface crack constructed in the model of ring part

3.1 Method 1

The method to calculate the stress intensity factor considering the changing of applied loads calculated by Eq. (1).

$$K_I = \left[G_0\sigma_0 + G_1\sigma_1\left(\frac{a}{t}\right) + G_2\sigma_2\left(\frac{a}{t}\right)^2 + G_3\sigma_3\left(\frac{a}{t}\right)^3 + G_4\sigma_4\left(\frac{a}{t}\right)^4\right]\sqrt{\frac{\pi a}{Q}} \quad (1)$$

$$Q = 1.0 + 4.593\left(\frac{a}{2c}\right)^{1.65} \text{ for } a/c \le 1 \quad (2)$$

where, K_I is the stress intensity factor of fracture model Ⅰ. G_0, G_1, G_2, G_3 and G_4 are the factors depending on the sizes and shapes of a surface crack, and among those factors, G_2, G_3 and G_4 are different at deepest with surface point of a surface crack. t is the thickness of ring wall. σ_0, σ_1, σ_2, σ_3 and σ_4 are the coefficients depending on Eq. (3). By fitting Eq. (3) to the axial stress within half length of the measured path by simulated as shown in Fig. 4, the coefficients of σ_0, σ_1, σ_2, σ_3 and σ_4 were obtained.

$$\sigma(x) = \sigma_0 + \sigma_1\left(\frac{x}{t}\right) + \sigma_2\left(\frac{x}{t}\right)^2 + \sigma_3\left(\frac{x}{t}\right)^3 + \sigma_4\left(\frac{x}{t}\right)^4 \quad (3)$$

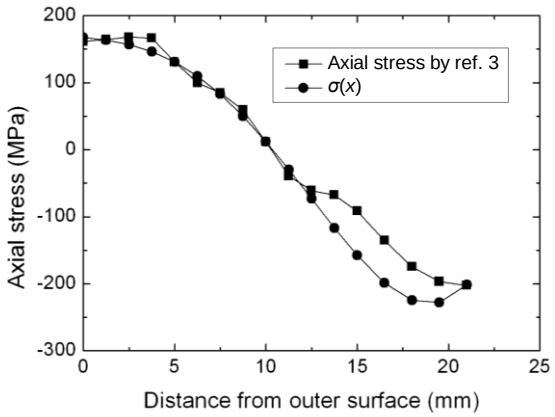

Fig. 4 Fitting load curve for solution of the coefficients of $\sigma_{0\text{-}4}$

3.2 Method 2

The other fitness-for-service method is using the experienced equations as shown in Eqs. (4-7), and can use the stress distribution at the tip of crack to calculate the stress intensity factor.

$$K_I = G_0^*\sigma\sqrt{\frac{\pi a}{Q}} \quad (4)$$

$$G_0^* = A_0 + A_1\beta + A_2\beta^2 + A_3\beta^3 + A_4\beta^4 + A_5\beta^5 + A_6\beta^6 \quad (5)$$

$$\beta = \frac{2\theta}{\pi} \quad (6)$$

$$Q = 1.0 + 1.464\left(\frac{a}{c}\right)^{1.65} \text{ for } a/c \le 1.0 \quad (7)$$

where, σ is the axial stress at crack tip obtained by simulation after introducing a static surface crack. G_0^* and A_{0-6} are the coefficients and dependent of ratios of a/t, c/a and depth of crack to thickness of cylinder. θ is the angle defined in Ref. 1, and $\theta = 0^\circ$ at the surface point of the crack and $\theta = 90^\circ$ at the deepest point.

4. RESULTS AND DISCUSSION

By the two methods, we calculated the stress intensity factor at the deepest point and surface point of the cracks, and the results were plotted in Figs. 5 and 6, respectively.

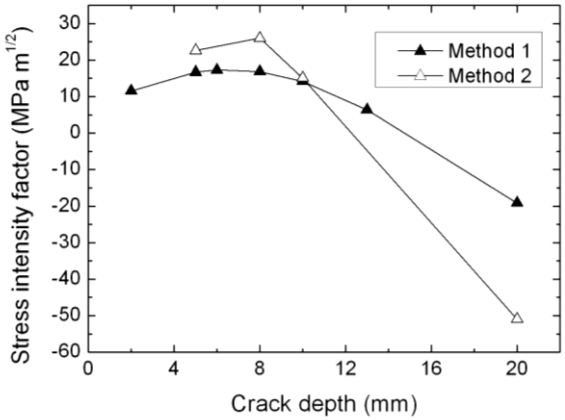

Fig. 5 Stress intensity factor at the deepest point of the surface crack with the propagation of crack

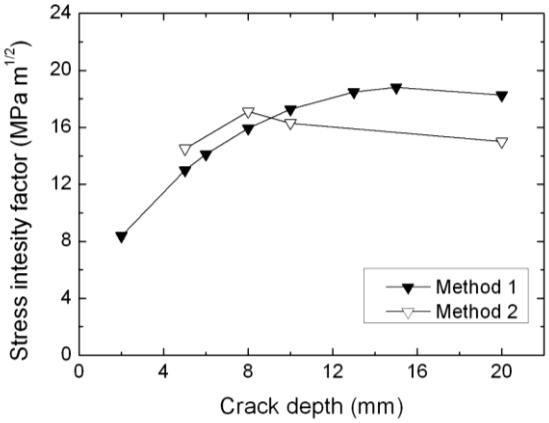

Fig. 6 Stress intensity factor at the surface point of the surface crack with the propagation of crack

At the deepest point of the surface crack, the stress intensity factor with method 1 increases to 17.3MPam$^{1/2}$ at crack depth of 6mm, and decreases to 0 MPam$^{1/2}$ at about 15mm. It decreases to -20MPam$^{1/2}$ until 20mm in crack depth. The calculated results at deepest point of the surface crack indicate that the propagation of

the surface crack is suspended at 15mm in the depth direction. Correspondingly, stress intensity factor by method 2 is an enlarged calculation result of stress intensity factor. Stress intensity factor increases with increase of crack depth and saturates in about 15mm in depth at the surface point in method 1 as shown in Fig. 6. As for the method 2, the same tendency is observed. This means that the surface crack propagates continuously in length direction with increasing crack length, which is well agreement with the results stress intensity factor in pipe and plate by Miyazaki *et al* [5].

However, the stress intensity factor at deepest point of crack by method 2 had much difference to that by method 1. From the comparison of the results using two polynomial equations (Eqs. (1) and (4)), the different estimated results were caused by the stress term at crack tip by the two methods as shown in Fig. 7. At surface point of the crack, the stress term is almost same for the two methods while it is enlarged in method 2 comparing with method 1. The current data of G_0^* in method 2 is defined by $a/t = 0.2$ in API RP579. When we used G_0 that used in method 1, the values of stress term much larger than that calculated by using G_0^*, as a result the estimated stress intensity factor in method 2 was enlarged much largely comparing with method 1. This indicates that the difference of the stress intensity factor by the two methods is caused by the enlarged axial stress at crack tip in method 2.

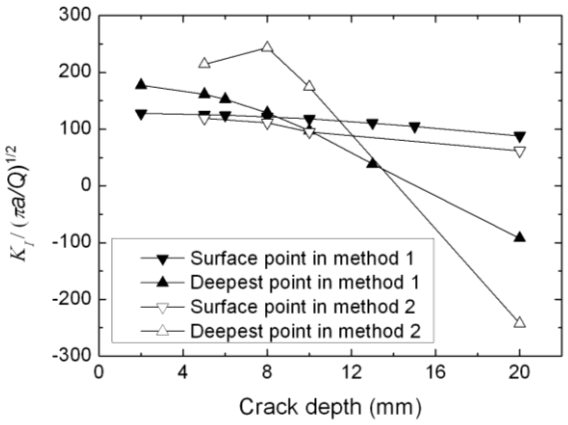

Fig. 7 Term of axial stress at deepest point and surface point of crack by simulation

The residual stress used in method 1 was tested for its reliability by using the method of release node ahead a crack with finite element method by Miyazaki *et al*[6]. However, the current component is not regular pipe. The same method of release node needs to be conducted on the ring model for high reliability of the evaluation of stress intensity factor. In the node release finite element method, the axial residual stress at the crack tip becomes very large while the redistribution of axial residual stress is not so apparent [6]. By using the residual axial stress at crack tip, the estimated results of stress intensity factor by method 2 must be larger than the current results. However, the estimated stress intensity factor by Miyazaki *et al* shows that the redistribution of axial residual stress does not affect the evaluation of stress intensity factor by J integral or method 1. For the load type of inner residual stress in a component, the other relative references of using method 2 to calculate the stress intensity factor are not found at present. Therefore, we conclude that the method 2 is not suitable for estimating stress intensity factor in the component of this study.

5. SUMMARY

Two calculation methods to stress intensity factor in API RP579 were used. Method 1 can be used for evaluation on the crack propagation behavior in present model with continuous testifying its reliability. Method 2 is not suitable for the estimation of the components under the residual stress.

REFERENCE

[1] Recommended Practice 579: Fitness-For-Service, 1st Ed. American Petroleum Institute: (2000).
[2] Li, Y., Kaji, Y. and Igarashi, T., Simulation of Residual Stress due to Welding in Core Shroud of Boiling Water Reactor, NO.100197 of Spring AESJ, Mito, (2010).
[3] Li, Y., Kaji, Y. and Igarashi, T., Study of Weld Residual Stress Field in the Girth Seam H6a of Core Shroud of Boiling Water Reactor, Proceeding of the 18th International Conference on Nuclear Engineering, Xi'an, China (2010).
[4] Simulia, ABAQUS User Manual, Version 6.9, (2009).
[5] Miyazaki, K., Mochizuki, M., Effects of Residual Stress Distribution and Geometry of Components on Stress Intensity Factor and Crack Growth Behavior of Surface Crack, Quarterly Journal of the JWS, (2006), p78-86.
[6] Miyazaki, K., Numata, M., Saito, K., and Mochizuki, M., Effects of Distance from Center of a Weld to Fixed End on Residual Stress Intensity Factor of a Piping Weld, Quarterly Journal of Japan Welding Society, (2006), p70-77.